TNO-*report*
TPD-HAG-RPT-960094

Box-like seating structures; interface shape dependence

TNO Institute of Applied Physics

Stieltjesweg 1
P.O. Box 155
2600 AD Delft
The Netherlands

Phone (+31) 15 69 20 00
Fax (+31) 15 69 21 11

Date

October 1996

Author(s)

prof.dr. B.A.T. Petersson

Classification

Classified by	: ing. H. Hasenpflug
Classification date	: October 1996
	(After 10 years this classification is no longer valid)
Title	: Ongerubriceerd
Executive summary	: Ongerubriceerd
Abstract	: Ongerubriceerd
Report text	: Ongerubriceerd
Appendices A-B	: Ongerubriceerd

Copy no.	: 18
No. of copies	: 18
No. of pages	: 28 (including appendices, excluding distribution list)
No. of appendices	: 1

TNO Institute of Applied Physics (TPD) is a contract research organization for industry and government with a multi-disciplinary approach. In-house disciplines are: applied physics, information technology, mechanics, electronics, materials and process technology.

Netherlands organization for applied scientific research

MANAGEMENTUITTREKSEL

Titel	:	Box-like seating structures; interface shape dependence
Auteur(s)	:	prof.dr. B.A.T. Petersson
Datum	:	October 1996
Projectnr.	:	A95/KM/133
IWP-nr.	:	797
TPD projectnr.	:	627.200
Reportnr.	:	TPD-HAG-RPT-960094

Aanleiding tot het onderzoek
In werkgebied I van het TNO-DO onderzoekprogramma worden rekenmodellen ontwikkeld voor de beschrijving van constructiegeluidoverdracht van machines naar de scheepsconstructie via verschillende typen fundaties. Bij een studie naar de zogenaamde 'doos-achtige' fundatie (TPD-HAG-RPT-950092) bleek dat onvoldoende duidelijk was wat de invloed is van de vorm van het contactvlak tussen de fundatie en de scheepsconstructie op de geluidoverdracht.

Doel van het onderzoek
Het afleiden van analytische uitdrukkingen die beschrijven wat de invloed is op de geluidoverdracht van de vorm van het contactvlak tussen een 'doos-achtige' fundatie en scheepsconstructie.

Werkplan
Het uitvoeren van een analytische en numerieke modellering van het reële deel van de effectieve admittantie voor verdeelde aanstoting van een plaatachtige constructie via een rechthoekige rand. Onderzoeken van de invloed van de lengte-breedteverhouding van de rechthoek op de admittantie voor een uniforme spanningsverdeling ('nulde orde') en een lineair verlopende spanningsverdeling ('eerste orde'). De resultaten zullen worden vergeleken met eerder gevonden resultaten voor een cirkelvormig contactvlak (TPD-HAG-RPT-950024).

Conclusies
Het contactvlak mag als een punt worden beschreven zolang de omtrek van het contactvlak kleiner is dan de buiggolflengte in de ontvangende plaatconstructie. Bij grotere contactvlakken treedt uitmiddeling op, zodat de effectieve geluidoverdracht vermindert. Deze vermindering kan worden gekwantificeerd met behulp van de in dit rapport beschreven schattingsprocedures.

Contents

Preface

The present report concerning the influence of the interface geometry on an extended version of mobilities constitutes a part of the work within the mid-term defence research (DO–MLTP). It is the third part of a study of the mobility concept employed in cases where the excitation is distributed over some closed contour interface.

The author is grateful to Dr. C. deJong and Mr. F. v.d. Knaap, TNO Institute of Applied Physics, for pointing out the discrepancy between theoretical and experimental results which initiated the work.

The research has been sponsored by the TNO Defence Research Organization under the mid-term plan (contract A95/KM/133)

Loughborough University of Technology in April, 1996
Björn A.T. Petersson

1 Introduction

In some recent studies [1], [2], the dynamic interaction between a superstructure and the recipient for the vibrational energy has been considered. In particular, the cases with interfaces which are large in comparison with the governing wave length of the recipient require detailed consideration in order to circumvent the often rather cumbersome mixed boundary value problem implied. In [3], the important conclusion was drawn that for a large class of structural configurations pertinent to the shipboard structural acoustics transmission problem, essentially the zero and first order stress distributions suffice for the modelling. It was argued, moreover, that for not too extreme geometrical shapes of the interface, the annular interface constitutes the generic case. In subsequent experimental work [4] it has been observed, however, that deviations from calculated results were obtained, below and in the transition range from point-like to surface-like excitation for a rectangular interface and the question was posed whether those deviations could be explained by a shape dependence.
The interface problem underlying the aforementioned study, of course, is of central importance for superstructures such as machinery seatings which are installed on recipients for the vibratory energy, e.g. the bottom structure of ships. Interface mobilities of plate-like structures have been derived [5] for the case of annular shapes which show that for both the zero (transverse force) and first order (lateral force or moment) excitation distributions, the real parts equal those found for ordinary point excitation when the governing wavelength of the recipient is larger than the circumference of the interface and decrease markedly at high frequencies. The imaginary part of the zero order interface mobility is small and negative and can be termed a negative spring while that of the first order interface mobility is stiffness controlled in the region of point-like behaviour. Although the quantitative details may vary with the shape of the interface the overall character will remain the same. This means that with a mass controlled superstructure, the transmission may be enhanced due to matching but no system resonance will occur for transverse force excitation. If, on the other hand, the dynamic characteristics of the superstructure are stiffness controlled, a system resonance may occur because of the different signs of the imaginary parts involved. Such a system resonance, of course, can be very pronounced but then, affect a limited frequency region. For a lateral force or moment excitation, a mass-controlled behaviour of the superstructure will unavoidable lead to a system resonance whereas a stiffness-controlled behaviour, at worst, lead to a broad matching. In the experimental comparison referred to above, however, the deviations showed a reduced power transmission which can be explained by a markedly altered real part of the interface mobility in the rectangular case.
In order to investigate such a shape dependence, the transmission of vibrational power at a rectangular interface is addressed. The theoretical analysis is carried out for both a primary

transverse force excitation and a primary lateral force or moment excitation. As in the case of an annular interface, a plate-like recipient is assumed.

2 Analysis

2.1 Zero order excitation distribution

Consider a thin homogeneous, linearly elastic plate subject to an excitation distributed over a strip with an overall rectangular form as depicted in Figure 1. Since the primary objective of the present study is to clarify the influence of the shape of the interface for the power transmission, the real part of the mobility constitutes the appropriate quantity. Owing to the fact that the dimensions of the interface can be larger than the wavelength of the free flexural wave, however, the mobility concept must be extended. This is achieved by considering the so-called effective interface mobility, defined in [3]. As discussed in e.g. [6], a proper analytical model in the shipboard context, is realized by a recipient plate of infinite extent.

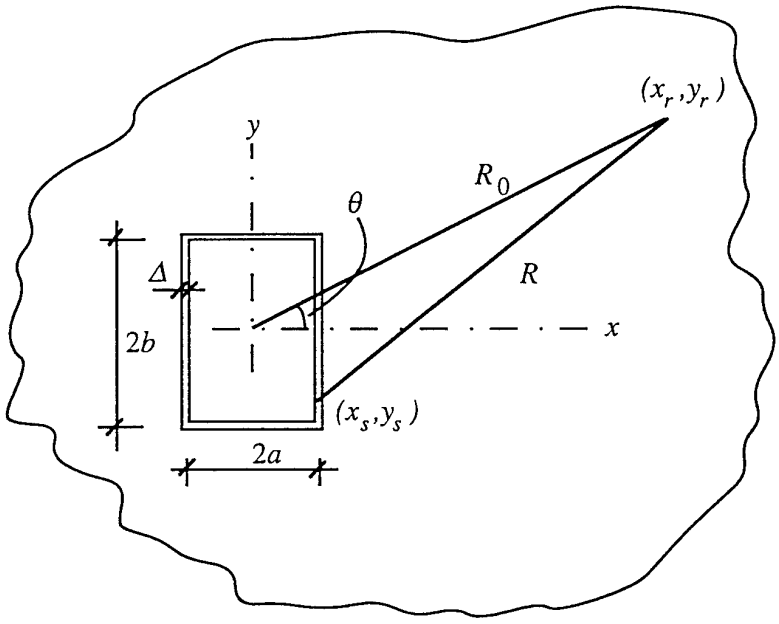

Figure 1: A thin plate excited over a rectangularly shaped strip.

For the sake of physical rigour, the strip is assumed to be of finite width and the stress to be uniformly distributed both along and across the strip-like interface, see Figure 2.

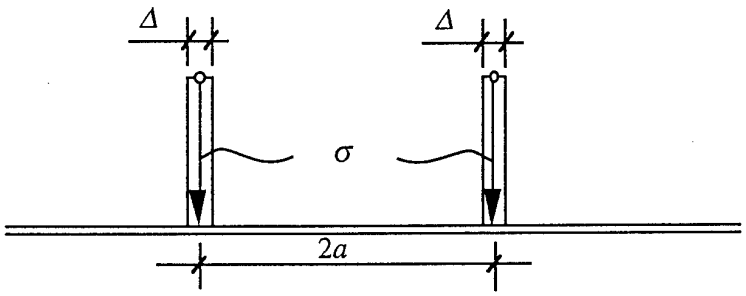

Figure 2: Cross-section of strip distributed excitation.

Therefore, let the zero order stress be given by,

$$\sigma = \frac{F_0}{4\Delta(a+b)} \quad . \tag{1}$$

For a thin infinite plate, the velocity due to a distributed excitation can be written [7]

$$v(x_r, y_r) = Y^{\infty} \iint_S \sigma(x_s, y_s) E(k_B R) dS \quad , \tag{2}$$

where $Y^{\infty} = \omega / 8B'k_B^2$ is the ordinary point force mobility of an infinite plate and

$$E(kR) = H_0^{(2)}(kR) - H_0^{(2)}(-ikR) \quad . \tag{3}$$

Following [3], the real part of the interface mobility can be established by considering the far-field. For large distances between the excitation and an arbitrary response position, the propagation function above simplifies into

$$E(kR) \approx \sqrt{\frac{2}{\pi kR}} e^{-i(kR-\pi/4)} \quad . \tag{3a}$$

Moreover, under such conditions,

$$R^2 = x_r^2 - 2x_r x_s + x_s^2 + y_r^2 - 2y_r y_s + y_s^2 \quad ,$$

which can be approximated by

$$R^2 \approx R_0^2 \left(1 - 2\,x_s \cos\theta / R_0 - 2\,y_s \sin\theta / R_0\right) \quad , \tag{4}$$

or

$$R \approx R_0 - x_s \cos\theta - y_s \sin\theta \quad . \tag{4a}$$

This means that since essentially the phase is sensitive to the small geometrical perturbations,

$$v(R_0,\theta) \approx Y^{\infty} \frac{F_0 e^{i\pi/4}}{4\Delta(a+b)} \sqrt{\frac{2}{\pi k R_0}} \left\{ \int_{-a}^{a} \int_{-b}^{b} e^{-ik(R_0 - x_s\cos\theta - y_s\sin\theta)} dx_s dy_s \right.$$
$$\left. - \int_{-a+\Delta}^{a-\Delta} \int_{-b+\Delta}^{b-\Delta} e^{-ik(R_0 - x_s\cos\theta - y_s\sin\theta)} dx_s dy_s \right\} \quad .(5)$$

The integrations are readily obtained as

$$v(R_0,\theta) = Y^{\infty} \frac{F_0 e^{-i(kR_0 - \pi/4)}}{4\Delta(a+b)} \sqrt{\frac{2}{\pi k R_0}} \left\{ \left[\frac{2\sin(ka\cos\theta)}{k\cos\theta} \right] \left[\frac{2\sin(kb\sin\theta)}{k\sin\theta} \right] \right.$$
$$\left. - \left[\frac{2\sin(k(a-\Delta)\cos\theta)}{k\cos\theta} \right] \left[\frac{2\sin(k(b-\Delta)\sin\theta)}{k\sin\theta} \right] \right\} \quad .(6)$$

Since $\sin(\alpha-\beta) = \sin\alpha\cos\beta - \sin\beta\cos\alpha$, Eq. (6) can be rewritten as

$$v(R_0,\theta) \approx Y^{\infty} \frac{F_0 e^{-i(kR_0 - \pi/4)}}{\Delta(a+b)} \sqrt{\frac{2}{\pi k R_0}} \left\{ \left[\frac{\sin(ka\cos\theta)}{k\cos\theta} \right] \left[\frac{\sin(kb\sin\theta)}{k\sin\theta} \right] \right.$$
$$- \left[\frac{\sin(ka\cos\theta)\cos(k\Delta\cos\theta) - \sin(k\Delta\cos\theta)\cos(ka\cos\theta)}{k\cos\theta} \right] \times$$
$$\left. \left[\frac{\sin(kb\sin\theta)\cos(k\Delta\sin\theta) - \sin(k\Delta\sin\theta)\cos(kb\sin\theta)}{k\sin\theta} \right] \right\} \quad ,$$

where, for small Δ,

$$v(R_0,\theta) = Y^{\infty} \frac{F_0 e^{-i(kR_0 - \pi/4)}}{(a+b)} \sqrt{\frac{2}{\pi k R_0}} \left[a\cos(kb\sin\theta) \frac{\sin(ka\cos\theta)}{ka\cos\theta} \right.$$
$$\left. + b\cos(ka\cos\theta) \frac{\sin(kb\sin\theta)}{kb\sin\theta} \right] \quad . \tag{6a}$$

Hence, for $k\Delta$ less than, say, 0.1, the farfield is independent of the width of the strip interface.

A power balance can now be employed to determine the real part of the interface mobility,

$$W = \frac{1}{2}|F_0|^2 \,\mathrm{Re}[Y_0] = c_B R_0 m'' \int_0^{2\pi} |v(R_0,\theta)|^2 d\theta \quad , \tag{7}$$

yielding

$$\mathrm{Re}[Y_0] = \frac{Y^\infty}{2\pi(a+b)^2} \int_0^{2\pi} \left[a\cos(kb\sin\theta)\frac{\sin(ka\cos\theta)}{ka\cos\theta} + b\cos(ka\cos\theta)\frac{\sin(kb\sin\theta)}{kb\sin\theta} \right]^2 d\theta \quad . \tag{8}$$

Let $p = 4(a+b)$ be the perimeter, see Figure 1, then the alternative form of the interface mobility is obtained as

$$\mathrm{Re}[Y_0] = \frac{8}{\pi} Y^\infty \int_0^{2\pi} \left[\frac{a}{p}\cos\left(kp\frac{b}{p}\sin\theta\right)\frac{\sin\left(kp\frac{a}{p}\cos\theta\right)}{kp\frac{a}{p}\cos\theta} + \frac{b}{p}\cos\left(kp\frac{a}{p}\cos\theta\right)\frac{\sin\left(kp\frac{b}{p}\sin\theta\right)}{kp\frac{b}{p}\sin\theta} \right]^2 d\theta \quad . \tag{9}$$

To get an analytical overview, the integrands can be expanded in terms of $\sin\theta$ and $\cos\theta$ which for $ka << 1$ and $kb << 1$ leads to,

$$\mathrm{Re}[Y_0] \approx \frac{Y^\infty}{2\pi(a+b)^2} \int_0^{2\pi} \left\{ (a+b)^2 - 2(a+b)k^2 \left[\frac{a^2}{6}(3b+a)\cos^2\theta + \frac{b^2}{6}(3a+b)\sin^2\theta \right] \right\} d\theta \quad ,(8a)$$

and as a limit one finds,

$$\mathrm{Re}[Y_0] \to Y^\infty \left[1 - \frac{k^2}{6}(a+b)^2 \right] = Y^\infty \left[1 - \frac{k^2}{96}(4(a+b))^2 \right] \quad . \tag{9a}$$

This is to be compared with that of the annular case [5] i.e.,

$$\mathrm{Re}[Y_0] = Y^\infty \left(J_0(kr_0)\right)^2 \to Y^\infty \left[1 - \frac{k^2}{8\pi^2}(2\pi r_0)^2 \right] \approx Y^\infty \left[1 - \frac{k^2}{80}(2\pi r_0)^2 \right] \quad , \tag{10}$$

and it is seen that the decrease of the interface mobility compared with the ordinary point force mobility is slightly larger in the annular case than in the case of a rectangular strip for the same perimeter as schematically illustrated in Figure 3.

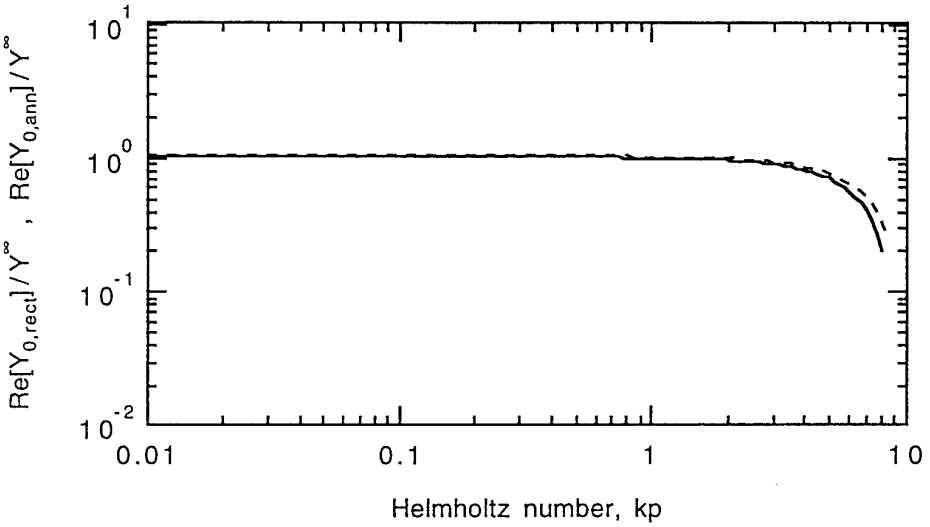

Figure 3: Schematic comparison of asymptotic behaviour of annular (————) and rectangular (- - - - -) interface mobility for the same perimeter p.

Rewriting the mobility as a function of Helmholtz number, ka, means that the asymptotic behaviour for small Helmholtz numbers is captured by

$$\mathrm{Re}[Y_0] \to Y^\infty \left[1 - \frac{(ka)^2}{6} \left(1 + (b/a)^2 \right) \right] \quad , \tag{11}$$

which can be used in a comparison of the influence of different shapes of the rectangular strip.

In Figure 4 is displayed the interface mobility versus Helmholtz number for various aspect ratios b/a. It is clearly seen that the onset of the reduction is controlled by the aspect ratio and that a decade increase in the aspect ratio means a shift of a decade downwards in Helmholtz number of the onset.

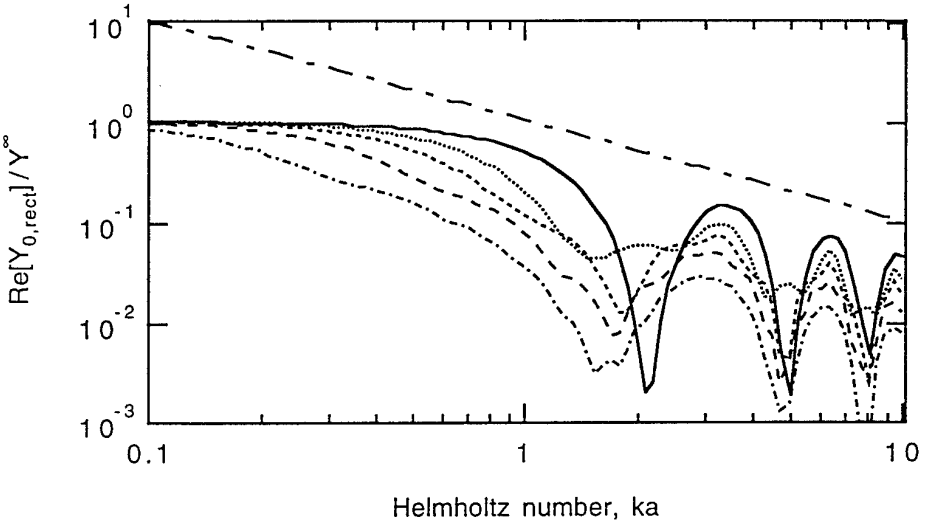

Figure 4: Interface mobility versus Helmholtz number based on side length for some aspects ratios: $b/a = 1$ (————), $b/a = 2$ (·····), $b/a = 3$ (- - - - -), $b/a = 5$ (— —) and $b/a = 10$ (-·-·-·-). Slope of characteristic beam mobility (— - —)

In order to assess the applicability of the approximation in Eq. (11), the results are compared with those obtained numerically using Eq. (8). In Figure 5 is shown the transition region and

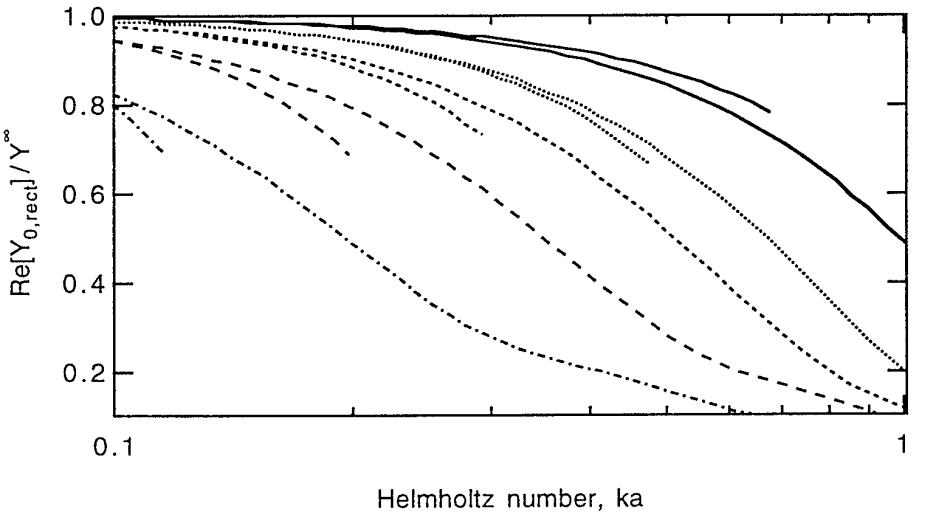

Figure 5: Asymptotic behaviour of the interface mobility for some aspects ratios: $b/a = 1$ (————), $b/a = 2$ (·····), $b/a = 3$ (- - - - -), $b/a = 5$ (— —) and $b/a = 10$ (-·-·-).

it emerges that the approximation for small Helmholtz numbers is applicable in the range below $ka < 1/(1+b/a)$ but deviates markedly from the integrated results above this limit.
A perhaps more adapted way of displaying the variation in interface mobility with aspect ratio is as function of Helmholtz number based on the perimeter, used in Figure 6.

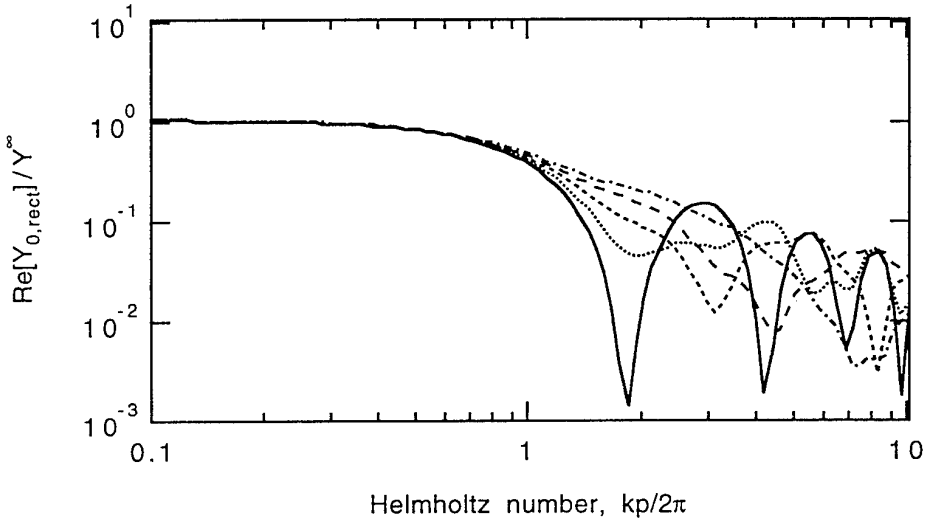

Figure 6: Interface mobility versus Helmholtz number based on perimeter for some aspects ratios: $b/a = 1$ (————), $b/a = 2$ (·····), $b/a = 3$ (- - - - -), $b/a = 5$ (— —) and $b/a = 10$ (-·-·-·-).

Here, as indicated in Figure 3, it is evident that, when the perimeter equals a wavelength of the governing wave, the spatial matching of the free wave and the excitation distribution starts to deteriorate and the real part of the interface mobility diminishes irrespective of the aspect ratio. Hence, the tentative conclusion drawn in [5] is strongly corroborated for this excitation distribution and accordingly the perimeter-wavelength criterion appears applicable for the onset of the influence of the distributed excitation.
The more or less deep troughs, of course, stem from the fact that power circulation occurs between the sides of the rectangular interface. Only in the case of a square-shaped strip interface, the pattern is regular.
Since, as illustrated in Figure 4, the envelope for the upper range of Helmholtz numbers follows a square root law it is possible to establish a simple estimation procedure as depicted in Figure 7. For the upper range, the estimates will be conservative. By shifting the onset of the inverse square root dependence to $kp/2\pi = 1/2$, the estimation in the upper range is somewhat improved.

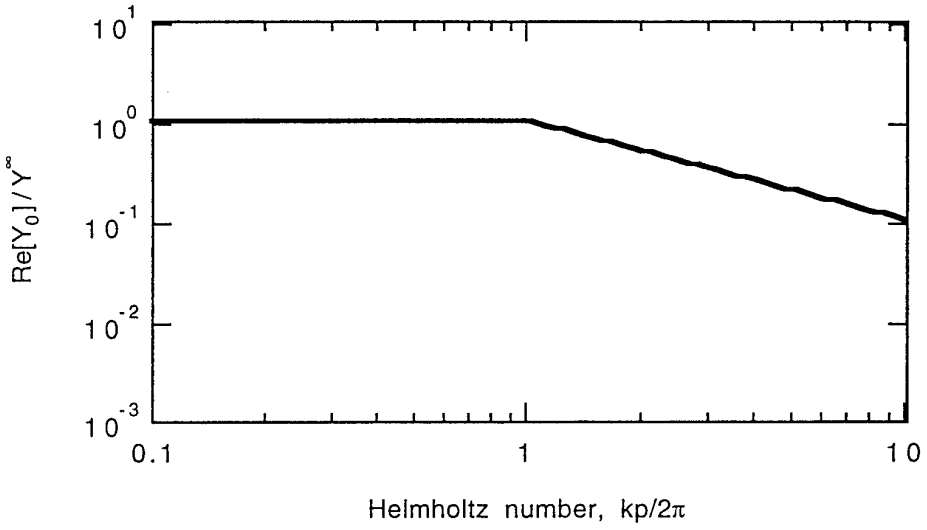

Figure 7: Estimation procedure for the zero order real part of interface mobility of closed contour strip interfaces.

2.2 First order excitation distribution

For this case as well, the strip is assumed to be of finite width but the stress to be linearly distributed in the x- or y-directions and to have a uniform distribution along the remaining strips, see Figure 8.

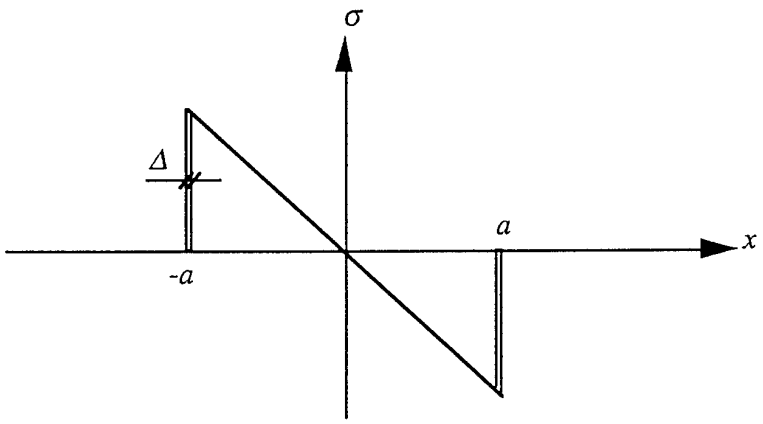

Figure 8: Cross-section of strip distributed moment excitation.

Therefore, let the stress take the form

$$\sigma(x,y) = -\frac{M_0}{4a(a/3+b)\Delta}\begin{cases}\text{sign(a)}\,; & -b \le y \le b\,,\ |x| = a \\ \dfrac{x}{a}\,; & -a \le x \le a\,,\ |y| = b\end{cases} \qquad (12)$$

As in the previous sub-section, a power balance is employed and leads to,

$$W = \frac{1}{2}|M_0|^2\,\mathrm{Re}[Y] = c_B R_0 m'' \int_0^{2\pi} |v(R_0,\theta)|^2 d\theta \qquad (13)$$

from which the real part of the first order interface mobility is formally found to obey,

$$\mathrm{Re}[Y_1] = \frac{4c_B m''}{\pi k |M_0|^2}\left(Y^{\infty}\right)^2 \int_0^{2\pi}\left|\int_{-a}^{a}\int_{-b}^{b}\sigma(x_s,y_s)\, e^{-ik(R_0 - x_s\cos\theta - y_s\sin\theta)} dx_s dy_s\right|^2 d\theta \qquad (14)$$

The inner integrations are readily obtained as,

$$I = 4i\left\{ b\sin(ka\cos\theta)\left[\frac{\sin(kb\sin\theta)}{kb\sin\theta}\right] + a\cos(kb\sin\theta)\left[\frac{\sin(ka\cos\theta)}{(ka\cos\theta)^2} - \frac{\cos(ka\cos\theta)}{ka\cos\theta}\right]\right\} \quad .(15)$$

The real part of the first order interface mobility thus becomes,

$$\mathrm{Re}[Y_1] = \frac{Y^\infty}{2\pi(a/3+b)^2}\int_0^{2\pi}\left[\frac{b}{a}\sin(ka\cos\theta)\left[\frac{\sin(kb\sin\theta)}{kb\sin\theta}\right] + \cos(kb\sin\theta)\left[\frac{\sin(ka\cos\theta)}{(ka\cos\theta)^2} - \frac{\cos(ka\cos\theta)}{ka\cos\theta}\right]\right]^2 d\theta \quad ,(16)$$

which also is independent of the width of the strip interface for small enough $k\Delta$.
As for the uniform stress, the integrand can be expanded in terms of $\sin\theta$ and $\cos\theta$ to get an analytical overview which for $ka << 1$ and $kb << 1$ leads to,

$$\mathrm{Re}[Y_1] \approx \frac{Y^\infty k^2}{2\pi(a/3+b)^2}\int_0^{2\pi}\left\{(b+a/3)^2\cos^2\theta - \frac{k^2}{3}\cos\theta(b+a/3)\left[b\cos\theta\left(b^2\sin^2\theta + a^2\cos^2\theta\right) - a\cos\theta\left(\frac{a^2}{5}\cos^2\theta + b^2\sin^2\theta\right)\right]\right\} d\theta \quad ,$$

and after integration, the asymptotic behaviour is found to be

$$\mathrm{Re}[Y_1] \to Y^\infty\frac{k^2}{2}\left\{1 - \frac{k^2 ba}{180(a/3+b)^2}\left[3a^2(8+a/b) + 5b^2(4+3b/a) + 50ba\right]\right\}. \quad (17)$$

As expected, the real part of the first order interface mobility converges towards that of the ordinary point moment mobility as the wavenumber and the dimensions decrease. It is clear from Eq.(17) however, that the dependence on the aspect ratio is more involved than in the case of a uniform stress. Indeed, the asymptote demonstrates an area dependence. The real part of the first-order interface mobility for the rectangular case can be compared with that of the annular case, i.e.,

$$\mathrm{Re}[Y_1]= 2Y^{\infty}\left(\frac{J_1(kr_0)}{r_0}\right)^2 \rightarrow \frac{k^2}{2}Y^{\infty}\left[1-\frac{(kr_0)^2}{4}\right] \approx \frac{k^2}{2}Y^{\infty}\left[1-\frac{(kp)^2}{158}\right], \qquad (18)$$

and so by rewriting Eq. (17) as,

$$\mathrm{Re}[Y_1] \rightarrow Y^{\infty}\frac{k^2}{2}\left\{1-\frac{(ka)^2 b/a}{180(1/3+b/a)^2}\left[3(8+a/b)+5(b/a)^2(4+3b/a)+50b/a\right]\right\} \qquad ,(17a)$$

it is seen that for $a=b$ and letting a correspond to the radius r_0, the rectangular case implies a smaller mobility;

$$\mathrm{Re}[Y_1] \rightarrow \frac{k^2}{2}Y^{\infty}\left\{1-\frac{7}{15}(ka)^2\right\} \approx \frac{k^2}{2}Y^{\infty}\left\{1-\frac{(kp)^2}{137}\right\}$$

In contrast to the case with a uniform stress excitation, it is seen that the decrease of the present interface mobility, normalised with respect to the ordinary point moment mobility, is slightly smaller in the annular case than in the case of a rectangular strip for the same perimeter. This schematically illustrated in Figure 9.

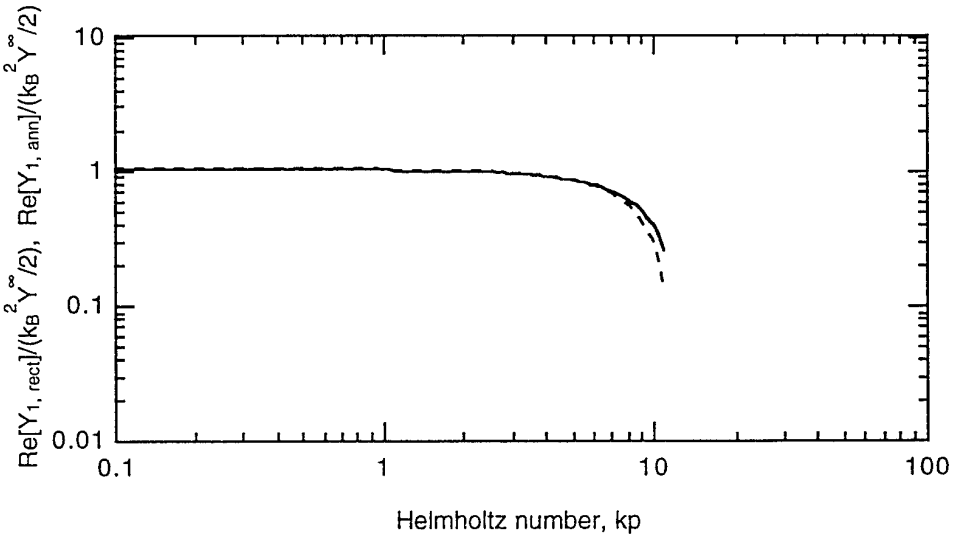

Figure 9: Schematic comparison of asymptotic behaviour of annular (———) and square-shaped (- - - - -) first order interface mobility for the same perimeter p.

In Figure 10 is displayed the interface mobility versus Helmholtz number, based on the short side length, for various aspect ratios b/a. It is seen that the onset of the reduction is controlled by the aspect ratio and that a decade increase in the aspect ratio means a shift of a decade downwards in Helmholtz number of the onset. One can note, however, that the signature in the upper range is more regular than that of the uniform stress.

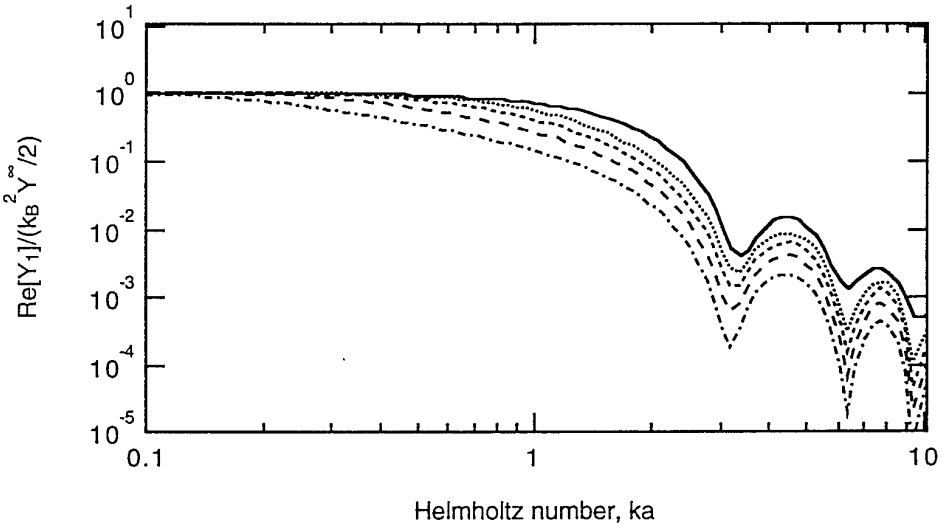

Figure 10: Interface mobility versus Helmholtz number based on side length for some aspects ratios: $b/a = 1$ (———), $b/a = 2$ (·····), $b/a = 3$ (- - - - -), $b/a = 5$ (— —) and $b/a = 10$ (-·-·-·).

In Figure 11 is visualised the range of validity of the asymptotes developed for small Helmholtz numbers. Again, the approximation given by Eq. (17a) is applicable in the range below $ka < 1/(1+b/a)$ and deviates markedly from the integrated results in the range above. The adapted presentation of the first order interface mobility as function of Helmholtz number based on the perimeter, is given in Figure 12. It is again observed that the onset of the reduction in real part occurs when the perimeter equals the wavelength of the governing wave.

Owing to the fact that the first order excitation distribution is only single symmetric, it is necessary to numerically analyse also the influence of the shape of the interface for aspect ratios smaller than unity. In Figure 13 are shown the real parts of the moment interface mobilities for some aspect ratios smaller than unity.

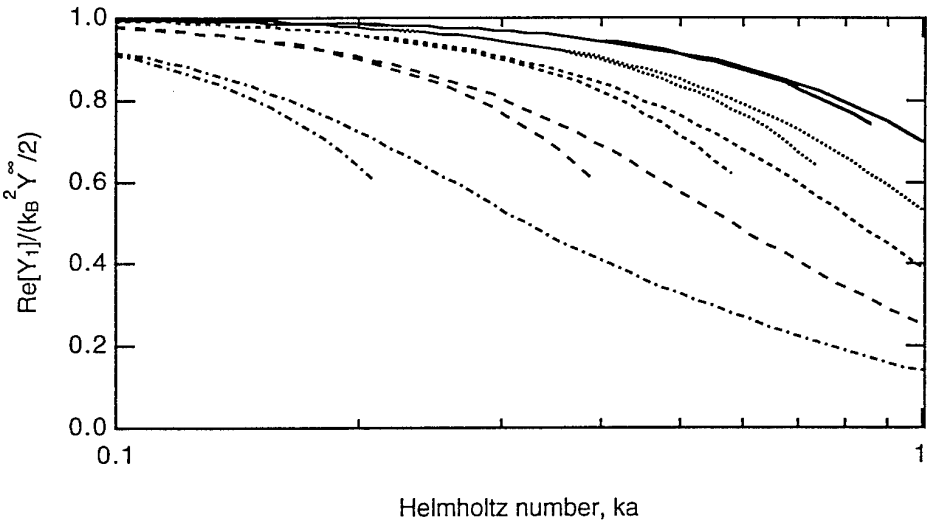

Figure 11: Asymptotic behaviour of the interface mobility for some aspects ratios: $b/a = 1$ (———), $b/a = 2$ (·····), $b/a = 3$ (- - - - -), $b/a = 5$ (— —) and $b/a = 10$ (-·-·-·-).

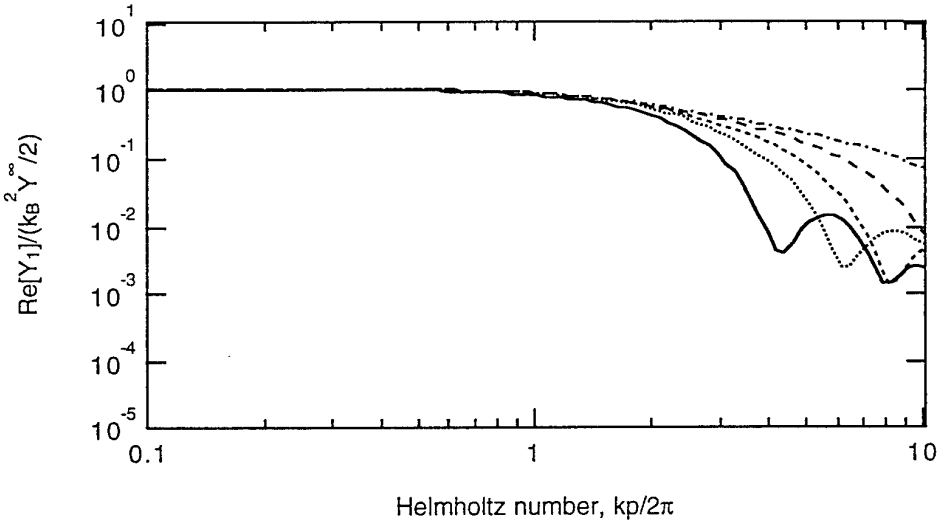

Figure 12: Interface mobility versus Helmholtz number based on perimeter for some aspects ratios: $b/a = 1$ (———), $b/a = 2$ (·····), $b/a = 3$ (- - - - -), $b/a = 5$ (— —) and $b/a = 10$ (-·-·-).

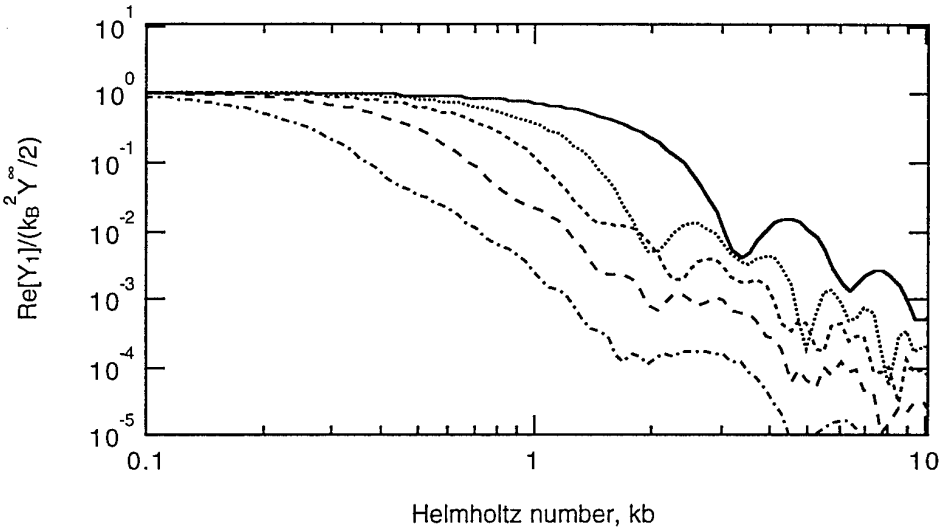

Figure 13: Interface mobility versus Helmholtz number based on perimeter for some aspects ratios: $b/a = 1$ (———), $b/a = 1/2$ (·····), $b/a = 1/3$ (- - - -), $b/a = 1/5$ (— —) and $b/a = 1/10$ (-·-·-).

It is seen that when the aspect ratio becomes smaller than unity, i.e. the interface becomes long in the direction perpendicular to the moment, the pattern of constructive and destructive is irregular, cf. Figure 10. Although such a trend is indicated also for the zero order distribution it is comparatively pronounced for the first order distribution owing to the basically elliptical field in the plate. The irregularity thus stems from the fact that here, sections of the interface stress can interfere when the long direction of the interface is perpendicular to the major axis of the elliptical field.

The asymptotic behaviour for small Helmholtz numbers, however, is still valid as seen in Figure 14. Of course it must be noted that when Helmholtz number is based on half the side length, b, the region of validity is given by $kb \leq 1/(1 + a/b)$.

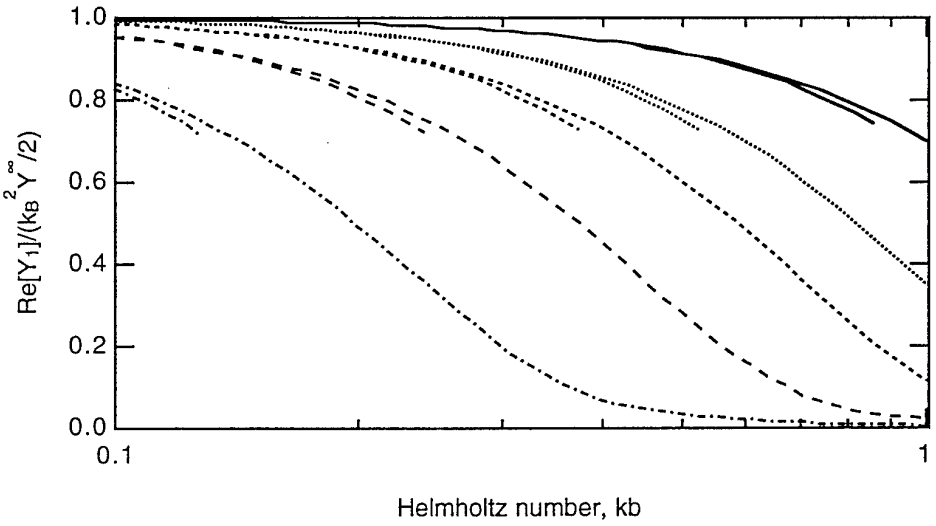

Figure 14: Asymptotic behaviour of the interface mobility for some aspects ratios: $b/a = 1$ (———), $b/a = 1/2$ (·····), $b/a = 1/3$ (- - - - -), $b/a = 1/5$ (— —) and $b/a = 1/10$ (-·-·-).

For the sake of completeness, the interface mobility is displayed also as function of Helmholtz number based on the perimeter, see Figure 15.

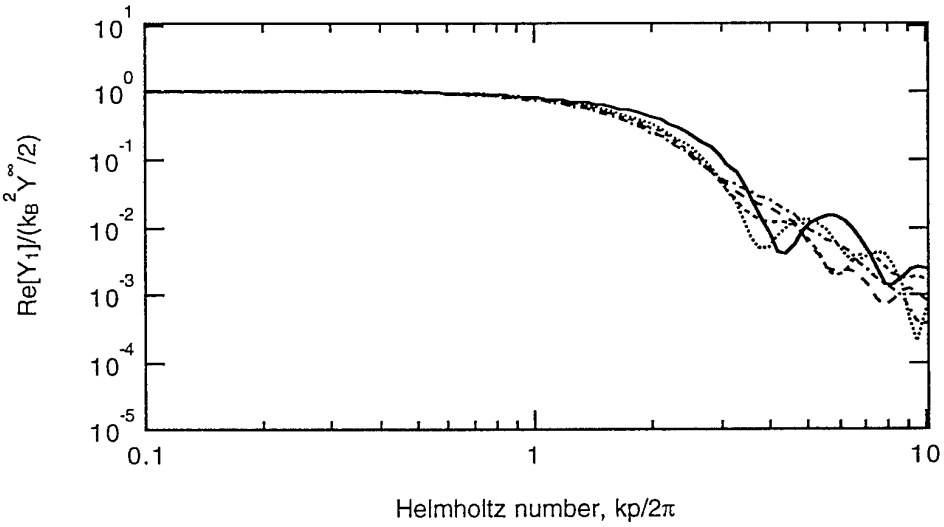

Figure 15: Interface mobility versus Helmholtz number based on perimeter for some aspects ratios: $b/a = 1$ (———), $b/a = 1/2$ (·····), $b/a = 1/3$ (- - - - -), $b/a = 1/5$ (— —) and $b/a = 1/10$ (-·-·-).

Accordingly, when the aspect ratio falls below unity, the normalised interface mobilities versus Helmholtz number based on the perimeter cluster and the aspect ratio i.e. the shape becomes more or less irrelevant provided the interface is long in the direction perpendicular to the moment vector.

As for the zero order interface mobility, one may rather easily identify the overall trends of the first order interface mobility. If one lets the length of the rectangular interface become very large in the direction of the moment, then the problem approach a two-dimensional counterpart i.e., a line moment on a plate. In such a case the slope is proportional to the square root of frequency. As the wavelength approach the length of the short side of the rectangular interface, the spatial mismatch between the excitation and the wave field increases markedly and a reduction in the power transmission is obtained. In this region therefore the slope becomes inversely proportional to the square root of frequency, as demonstrated in [5]. The added complication with an estimation procedure for the first order interface mobility hence, is the transition point between the two upper regions. As discussed in conjunction with Eq. (17), a direct relationship does not exist between the mobility and the aspect ratio nor the perimeter but a combined dependence on aspect ratio and the area enclosed is found. By focusing on the range of the aspect ratio $b/a < 5$, however, a reasonably straight-forward procedure can be established from the critical point where the length of the short side of the rectangular interface equals a wavelength. This means that the estimation procedure can be summarised as,

$$\mathrm{Re}[Y_1] \approx \begin{cases} Y^{\infty} \dfrac{(kp)^2}{2p^2}\,; & kp/2\pi \le 1\,;\ b/a \le 5 \\ Y^{\infty} \dfrac{\pi}{p^2} kp\,; & 1 \le kp/2\pi \le \pi b/a\,;\ 1 \le b/a \le 5 \\ 4Y^{\infty} \dfrac{\pi^3}{p^2} \dfrac{1}{kp}\,; & \pi b/a \le kp/2\pi\,;\ b/a \le 5 \end{cases} \tag{19}$$

In Figure 16, the results using the estimation procedure are compared with the calculated results for the limiting case $b/a = 5$. It is seen that the overall signature of the first order interface mobility is captured by the simple procedure although minor under- and overestimations are obtained in limited regions.

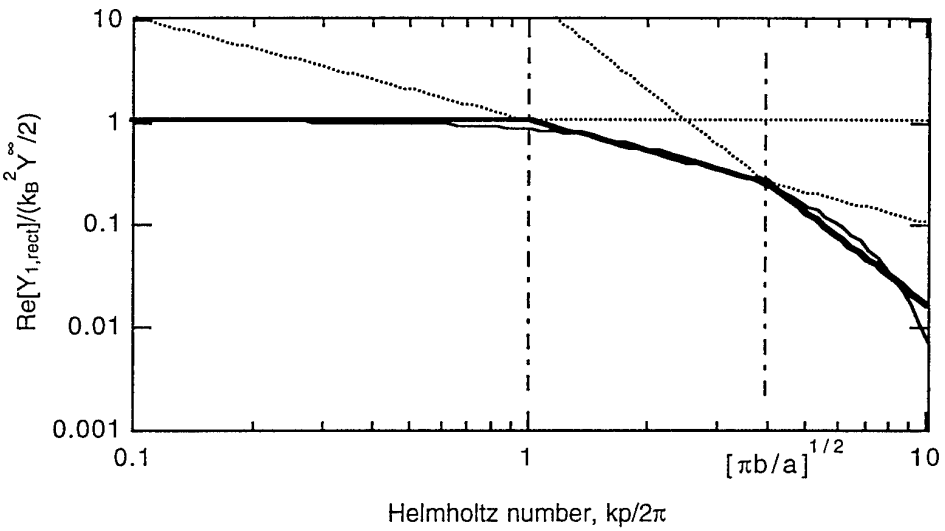

Figure 16: Estimation procedure for the real part of first order interface mobility of closed contour strip interfaces, displayed for $b/a = 5$. (———) $\mathrm{Re}[Y_1(b/a=5)]$, (.....) generating curves.

This means that when the aspect ratio is in the range of $1 \leq b/a \leq 5$, the first order interface mobility has three distinct regions, a first in which the ordinary point moment mobility gives an adequate description, an intermediate in which the principal behaviour is that of a moment excited beam and finally, an upper region in which the interface mobility is markedly reduced compared with plate moment mobility. As the aspect ratio falls below unity, the intermediate region vanishes and the first, constant region joins the third, steep region. For aspect ratios larger than five the uppermost, steep region can be omitted if the range of interest is below the upper transition point, approximately given by $kp \approx 2\sqrt{\pi^3 b/a}$.

3 Discussion and concluding remarks

The influence of interface geometry on the transmission of vibrational power from a superstructure to a recipient has been studied. The limited effect, previously heuristically inferred, is theoretically confirmed. It can thus be concluded that as long as the perimeter is less than the wavelength of the governing wave in the recipient, the ordinary point quantities are valid. For larger Helmholtz numbers where the perimeter is larger than the wavelength, the real part of the interface mobility exhibits more or less pronounced, rounded maxima and sharp minima set by the constructive and destructive interferences at the enclosed area of the plate. The envelopes to the zero and first order interface mobilities, in the case of a hollow rectangular interface, are those obtained for an annular one [5].

In this study, focusing on the vibration transmission, the imaginary part of the interface mobility is not treated explicitly. This is so, foremost, because at large Helmholtz numbers, this part is sensitive to the details of the interface geometry as well as the stress distribution cf. [8] and thus any result is valid merely for a specific configuration. Qualitatively, however, the behaviour for large Helmholtz numbers are those of the annular case when the aspect ratio of the rectangular interface is not extreme, typically less than 3, and tends to that of the strip mobility [9] for large aspect ratios. This means that in a broad-band sense, the transmission is controlled by the real part of the interface mobility. Therefore, it is not likely that the overall deviations from calculated results noted in the experimental work on a large freely suspended plate are due to an interface shape dependence [4]. The experimental results reported therein for a rectangularly shaped box with an aspect ratio of 1.5, however, showed no pronounced minima, as is predicted for an annular or square-shaped interface. As displayed in Figure 6, this feature is reduced for aspect ratios larger than unity which demonstrates that such destructive interference effects are indeed dependent upon the shape of the interface.

The zero order interface mobility is, qualitatively as well as quantitatively, practically independent of shape provided the perimeter is retained and the aspect ratio is close to unity. As the aspect ratio grows large, the interface mobility approaches that of a point excited beam, again largely irrespective of shape. Accordingly, these two trends constitute a conservative basis for an estimation procedure.

In contrast, the first order mobility for a rectangular interface must be treated differently for aspect ratios larger and smaller than unity respectively. In the former case, the interface mobility, at large Helmholtz numbers, tends to the corresponding beam mobility (moment excitation) whereas in the latter, the 'moment' interface mobility decreases as the force interface mobility, cf. [5]. This means that two different bases are required for an estimation procedure with respect to the first order interface mobility.

For a first order excitation it is not necessarily beneficial to design the interface long in the direction of the moment vector whereas it is always advantageous to increase the length in the direction across the moment vector.
For both the zero and first order distributions, there are more or less pronounced minima. In principle, such minima can be used for detuning the transmission for pronounced tonal components in the source descriptor. Although only the case with an aspect ratio of unity results in a regular pattern for all the minima, the pattern is well organised also for large aspects ratios already at the third minima. The exception is the first order interface mobility where a long interface across the moment vector reduces the significance of the local minima and establishes an irregular signature.

4 References

[1] B.A.T. Petersson, 1992. TNO Institute of Applied Physics, TPD-HAG-RPT-92-227. Point mobilities of column seatings: Theoretical basis and developments with respect to axial force excitation.

[2] B.A.T. Petersson, 1993. TNO Institute of Applied Physics, TPD-HAG-RPT-93-0215. Matched asymptotic mobilities - approximations for box-like seating structures.

[3] B.A.T. Petersson, 1992. TNO Institute of Applied Physics, TPD-HAG-RPT-92-110. Efficiency of annularly distributed moment and force excitation regarding structural acoustic power transmission to plate-like structures.

[4] C.A.F. de Jong & F.G.P. van der Knaap, 1995. TNO Institute of Applied Physics, TPD-HAG-RPT-950092. Input and transfer mobilities of a box-like seating structure; experiments and model calculations.

[5] B.A.T. Petersson, 1995. TNO Institute of Applied Physics, TPD-HAG-RPT-950024. Box-like seating structures: A study of geometrical and spatial interface effects.

[6] B.A.T. Petersson, 1991. TNO Institute of Applied Physics, TPD-HAG-RPT-91-191. A study of system definition in structure-borne sound and vibration problems.

[7] B.A.T. Petersson, 1990. Institute of Applied Physics, The Netherlands, TPD-SA-RPT-90-141. Moment excitation and structural acoustic power transmission between machinery and foundations; Part 2: Combined moment and force excitation of plate-like structures at or close to discontinuities.

[8] B.A.T. Petersson, 1994. TNO Institute of Applied Physics, TPD-HAG-RPT-940209. Point mobilities of thick plates and high beams: Descriptions of near-field effects.

[9] B.A.T. Petersson, 1993. TNO Institute of Applied Physics, TPD-HAG-RPT-93-0216. Surface excitation; part 1: Theoretical background and introductory study of beam- and frame-like systems.

Appendix I: Symbols and notation

B'	flexural stiffness per unit length
E	propagation function
F	force
H	Hankel function
I	integral
J	Bessel function
M	moment
R	radius
S	area
W	power
Y	mobility

a, b	half side length of interface
c	phase speed
i	imaginary unit
k	wavenumber
m''	mass per unit area
p	perimeter
v	translational velocity
w	rotational velocity
x, y, z	Cartesian co-ordinates

Δ	width of strip interface
α,β	auxiliary variables
θ	polar co-ordinate
ω	angular frequency
σ	normal stress

indices:

B	flexural
ann	annular
$rect$	rectangular
r	receiver
s	source

0	radius from interface centre, net external, zero order
1	first order

REPORT DOCUMENTATION PAGE (MOD-NL)

1. Defense report number (MOD-NL)	2. Recipient's accession number	3. Performing organization report number
RP-96-0208		TPD-HAG-RPT-960094
4. Project/Task/Work unit no.	5. Contract numbers	6. Report date
627.200	A95/KM/133	October 1996
7. Number of pages	8. Number of references	9. Type of report and dates covered
28	9	part report

10. Title and subtitle
Box-like seating structures; interface shape dependence

11. Author(s)
prof.dr. B.A.T. Petersson

12. Performing organization name(s) and address(es)
TNO Technisch Physische Dienst, Stieltjesweg 1, 2628 CK Delft

13. Sponsoring/monitoring agency name(s) and address(es)
TNO-Defense Research, Schoemakerstraat 97, 2628 CK DELFT
Ministry of Defence (Navy), Van der Burchlaan 31, 2597 PC 's-GRAVENHAGE

14. Supplementary notes
"ongerubriceerd" is equivalent to Unclassified

15. Abstract (maximum 200 words, 1044 byte)
The influence of the shape of the interface between a superstructure and a recipient on the vibrational energy transmission is analyzed. The real parts of the zero and first order interface mobilities are derived for a basic rectangular shape. Numerical results are presented for various aspect ratios but comparisons are also made with the corresponding results for an annular shape. It is concluded that the primary parameter is the perimeter of the interface and the condition that the wavelength is larger than the perimeter constitutes the transition from point to distributed contact. Also it is demonstrated that for closed-contour, strip-like interfaces, the real parts are independent of the strip width in a large and practically relevant range. With respect to the zero order interface mobility, the aspect ratio is of subordinate importance for the overall trend whereas the details of the signature are influenced. In contrast, the first order interface mobility includes two orthogonal cases, which are affected differently by the aspect ratio. Straightforward estimation procedures are developed for both interface mobilities.

16. Descriptors	identifiers
Vibration of elastic bodies, wave propagation	323F R14G

17a. Security classification (of report)	17b. Security classification (of page)	17c. Security classification (of abstract)
ongerubriceerd	ongerubriceerd	ongerubriceerd

18. Distribution/Availability statement	17d. Security classification (of titles)
Distribution according to agreed list. Additional availability via TNO-TPD (subject to TNO-DO and/or MOD/Navy approval).	ongerubriceerd

Distributielijst

1. DWOO *
2. HWO-CO **
3. HWO-KM **
4. HWO-KL **
5. HWO-KLu **
6. Ministerie van Defensie, Dir. Materieel KM, afdeling Scheepsbouw, ing. H. Hasenpflug.
7. Ministerie van Defensie, Dir. Materieel KM, afdeling Scheepsbouw, P. van der Gaag.
8. Ministerie van Defensie, Dir. Materieel KM, afdeling Scheepsbouw, ir. P.J. Keunig.
9. TNO-TPD-TU Delft, Hoofdafdeling Geluid, Afdelingsleider Geluidarm Construeren, ir. J.C. Vellekoop*.
10. TNO-TPD-TU Delft, Hoofdafdeling Geluid, Afdeling Geluidarm Construeren, dr.ir. C.A.F. de Jong*.
11. TNO-TPD-TU Delft, Hoofdafdeling Geluid, Afdeling Geluidarm Construeren, dr. B.A.T Petersson*.
12. TNO-TPD-TU Delft, Hoofdafdeling Geluid, Afdeling Geluidarm Construeren, ing. F.G.P. van der Knaap*.
13. TNO-TPD-TU Delft, Hoofdafdeling Geluid, Afdeling Geluidarm Construeren, prof.dr.ir. J.W. Verheij*.
14. TNO-DO*.
15. TNO-TPD-TU Delft, Hoofdafdeling Geluid, Archief*.
16. (t/m 18.) Bibliotheek KMA***

Indien binnen de krijgsmacht extra exemplaren van dit rapport worden gewenst door personen of instanties die niet op de verzendlijst voorkomen, dan dienen deze aangevraagd te worden bij het betreffende Hoofd Wetenschappelijk Onderzoek of indien het een K-opdracht betreft, bij de Directeur Wetenschappelijk Onderzoek en Ontwikkeling.

* Alijd een volledig rapport.

** Indien opdrachtgever een volledig rapport, anders een beperkt rapport.

*** 3 volledige rapporten indien het rapport ongerubriceerd of ongemerkt is, anders 1 volledig rapport.